Transient Kinetic Investigation of Chain Growth during CO Hydrogenation on Co/TiO_2 under Fischer-Tropsch Conditions: Elemental Balance of Species Adsorbed at the Catalyst Surface

Max Gäßler[a], Simon Hermann[a], Jens Friedland[a], Jakob Stahl[b], Lutz Mädler[b,c], Robert Güttel*[a]

[a] M. Gäßler, S. Hermann, Dr. J. Friedland, Prof. R. Güttel
Institute of Chemical Engineering
Ulm University
Albert-Einstein-Allee 11
D-89081 Ulm (Germany)
E-Mail: robert.guettel@uni-ulm.de

[b] J. Stahl, Prof. L. Mädler
Faculty of Production Engineering
University of Bremen
Badgasteiner Straße 1
D-28359 Bremen (Germany)Department

[c] Prof. L. Mädler
Leibniz Institute for Materials Engineering IWT
Badgasteiner Straße 3
D-28359 Bremen (Germany)

Supporting information for this article is given via a link at the end of the document.

Abstract: CO hydrogenation is a promising approach for the storage of renewable energy in the form of hydrocarbons via the Fischer-Tropsch synthesis (FTS). Since transient operation of FTS reactors might be necessary and even be beneficial, transient kinetics for a rational catalyst and reactor design are essential. In order to advance the development of such transient kinetics, the periodic transient kinetics (PTK) method was applied to the CO hydrogenation on a Co/TiO_2 catalyst under FT-like conditions. It was revealed that there are two carbon species of different reactivity, C_α and C_β, present on the catalyst surface during the reaction. C_α forms fast within a few seconds and is highly reactive, while C_β forms slowly, is accumulating on the surface over a longer time and imposes an inhibiting effect. However, a contribution of C_β to the chain growth reaction was shown. Finally, the transient experimental results are evaluated based on a material balance and the amounts of C_α and C_β present on the catalyst surface during the reaction were determined.

Introduction

In future energy supply systems, power-to-X (PtX) concepts can be incorporated as a solution for long-term energy storage of fluctuating renewable energy in form of high energy molecules, such as hydrogen, methane, or liquid hydrocarbons.[1,2] One possibility for the production of such molecules is the Fischer-Tropsch (FT) synthesis, where hydrogen from water electrolysis reacts with CO from renewable sources to form a wide spectrum of aliphatic hydrocarbons (see R1 – R2).[3]

$$n\,\mathrm{CO} + (2n+1)\mathrm{H_2} \rightleftharpoons \mathrm{C}_n\mathrm{H}_{2n+2} + n\,\mathrm{H_2O} \quad \text{R1}$$

$$n\,\mathrm{CO} + 2n\mathrm{H_2} \rightleftharpoons \mathrm{C}_n\mathrm{H}_{2n} + n\,\mathrm{H_2O} \quad \text{R2}$$

The CO hydrogenation is a heterogeneously catalyzed reaction and is usually carried out on supported transition metals, in particular Co, Fe and Ru, supported on various solid oxides, such as SiO_2, TiO_2, Al_2O_3 or CeO_2 among others.[4,5] Catalytic fixed-bed reactors, such as those used for FT synthesis, are usually operated in stationary mode. However, the dynamic operation might be beneficial for several applications.[6] For example, it was demonstrated that switching from a syngas feed to a H_2-rich feed increases production and selectivity towards the liquid fuel fraction (C_5 – C_{20}) by draining the liquid filled pores and decreasing mass transport limitations as well as the hydrogenolysis of wax (C_{20+}) filling the pores.[7] Furthermore, due to the volatile nature of renewable energies, a robust and efficient operation of FT reactors under fluctuating feed gas compositions is necessary.[8,9]

For the design of suitable reactors and catalysts, the reaction kinetics have to be known. However, we have already shown that conventional kinetics, derived under steady-state conditions, may fail to describe the CO hydrogenation under transient conditions.[10] Hence, transient kinetic models have to be developed, which consider processes such as ad-/desorption steps or surface reactions.[9,11] Micro-kinetic models, which take precisely these aspects into account, have already been used for the simulation of dynamic CO and CO_2 hydrogenation. However, these models require profound knowledge of the underlying reaction mechanism and sufficient experimental data for model parameterization.[11–14]

For this purpose, sophisticated transient experimental methods are necessary, which carry respective information on the dynamics of the involved reactions. Besides, transient methods have the advantage of being able to cover a wide range of operating conditions in a few experiments.[15] For example, steady-state isotopic transient kinetic analysis (SSITKA) is able to derive kinetic data by switching one reactant with its isotope.[16]

The transient response of the isotopically labeled species enables the determination of the amount of the active reaction intermediate, a mean surface residence time and can also demonstrate reversibility of surface reactions and was already applied to investigate the kinetics of the CO hydrogenation.[16–18] For instance, Vasiliades et al. used SSITKA in combination with operando diffuse reflectance infrared Fourier-transform spectroscopy (DRIFTS) measurements to investigate the nature of carbonaceous surface intermediates (C_α, C_β and C_γ) during CO hydrogenation on Co/Al_2O_3 catalysts.[19–21] However, in SSITKA only the isotopic composition changes are measured, while the system remains in steady-state. Hence, for the investigation of catalyst dynamics, SSITKA has to be combined with other transient methods. Consequently, Chen et al. used a combination of SSITKA and the chemical transient kinetics (CTK) method to investigate rate limiting steps in CO methanation and revealed that direct CO dissociation is more likely than H-assisted CO dissociation and that O hydrogenation is slow compared to CO dissociation.[22]

The CTK method involves the switching between two feed gas compositions, one containing synthesis gas and one containing hydrogen. In addition to the synthesis gas, a noble gas standard is fed into the reactor, which provides information about the residence time distribution (RTD), enabling the separation between residence time and kinetic effects.[23] The CTK method allows the investigation of reversible surface reactions as well as the balancing of the catalyst surface and the calculation of surface coverages for the individual elements.[24,25] We developed the periodic transient kinetics (PTK) method as an extension of CTK, by switching the feed gas composition periodically. After several switches, the system reaches a limit cycle, in which the individual periods only differ from another by noise. Averaging several periods within the limit cycle and applying statistical analysis provides a step response with a narrow confidence interval and high statistical significance.[26]

The goal of the present investigation is to provide the experimental basis for advancing a transient kinetic model for FT synthesis on Co catalysts. We use the PTK method to gather transient experimental data for the CO hydrogenation under FT-like conditions on a Co/TiO_2 model catalyst. We also quantify the carbon species C_α and C_β which are reversibly adsorbed on the catalyst surface. FT-like conditions are chosen, in order to ensure a certain degree of chain growth, which allows to investigate the influence of the different carbon species on the FT mechanism. At the same time, the formation of liquid hydrocarbons is suppressed to prevent mass transport limitations. Our results lay the foundation for subsequent mechanistic analysis of the transient processes and development of appropriate micro-kinetic models.

Experimental

Catalyst preparation and characterization

The Co/TiO_2 catalyst with a nominal Co-loading of 10 mol-% by metal was prepared as nano powder using double-flame spray pyrolysis[27] and sieved through a 250 µm mesh sieve to achieve homogenous agglomerate sizes as described in detail by Gäßler et al.[28] The catalyst is characterized by N_2 physisorption (BET), X-ray diffraction (XRD), transmission electron microscopy (TEM), energy dispersive X-ray (EDX) analysis, temperature-programmed reduction with hydrogen (H_2-TPR), and CO_2 chemisorption. The results of the H_2-TPR (figure S1) show two reduction peaks with their respective maxima at 340 °C and 390 °C. The XRD measurements revealed a crystalline phase composition of Co_3O_4 (ICSD: 97004), anatase-TiO_2 (ICSD: 172916) and rutile-TiO_2 (ICSD: 9161) with crystallite sizes of 7.2 ± 0.2, 21.0 ± 0.3 and 10.7 ± 0.2 nm for Co_3O_4, a-TiO_2 and r-TiO_2 respectively.[28] Further characterization results are summarized in table 1.

Table 1. Characterization results of Co/TiO_2 taken from Gäßler et al.[28]

Parameter	Value	Method
Co_3O_4 size / nm	8.0 ± 0.1	TEM
Co_3O_4 size / nm	7.2 ± 0.2	XRD
Elementary composition / mol-%	9.3 ± 1.0 Co / 90.7 ± 1.0 Ti	EDX
BET surface / $m^2\ g^{-1}$	86 ± 2	N_2 physisorption
Average particle size / nm	16.1 ± 0.3	N_2 physisorption
CO_2 sorption capacity / µmol g^{-1}	9.4 ± 1.2	CO_2 Chemisorption

Experimental setup and methodology

The experiments were carried out in a differential fixed-bed reactor consisting of a 1/4 in. stainless steel tube containing a 1/16 in. steel capillary for a movable thermocouple (Type K, TMH). The reactor setup is described in detail by Gäßler et al.[28]. The catalyst bed consists of 100 mg of catalyst material diluted by 200 mg of nonporous silica beads (150 – 250 µm) and was reduced *in situ* at 400 °C under pure H_2 for 12 h. The packing is held in place by 1 g of silica beads upstream and 0.6 g downstream and silica wool in between the layers. The total packing length sums up to 12 cm, with a catalyst bed length of 2 cm. The catalyst bed is placed in an isothermal zone, monitored by measuring the axial temperature profile. The pressure in the setup was regulated by two high precision back pressure regulators (LF1 Equilibar). The analytics consisted of a mass spectrometer (MS, MKS Cirrus 3XD), calibrated to the mass-to-charge ratios 2 (H_2), 4 (He), 15 (CH_4), 18 (H_2O), 20 (Ne), 26 (C_2), 28 (CO), 40 (Ar) and 43 (C_3). Ethane and Ethylene were pooled together, as we were unable to distinguish them in the MS. The same applies to C_{3+}, with the major contributors C_3H_8 and C_4H_{10}. The MS measurement was validated via an on-line gas chromatograph (GC, Shimadzu GC2010), by performing a steady-state measurement at the same operating conditions, before each PTK experiment.

Prior to the transient experiments, steady-state experiments are performed in order to identify FT-like conditions under which certain degree of chain-growth is achieved, while the formation of significant amounts of liquid products can be neglected. The reactor effluent was analyzed by GC, with respect to all gaseous

compounds, including all hydrocarbons up to a carbon number of 6. The gas composition measured after 4 h time on stream (TOS) was used as reference point to ensure comparability. The experiments under FT-like conditions were carried out in a separate test plant with a similar reactor setup, but with additional hot and cold traps to ensure absence of condensed liquid hydrocarbons.

After a suitable operating point was identified, the dynamic behavior of the CO-hydrogenation was investigated using the experimental setup and methodology described in detail by Meyer et al.[10,26,29] and Gäßler et al.[28], using the PTK method. The PTK method involves periodic step changes between two feed gas compositions and analysis of the gas composition at the reactor outlet via MS with a high temporal resolution of 0.5 s. The compositions in the feed gas lines were adjusted via MFCs (Bronkhorst EL-Flow Prestige) and can provide H_2, He, Ar, and CO. The switching was executed via a pressure actuated high-speed valve (FITOK Boss) and was assumed to be an ideal step, as the switching process was faster than the temporal resolution of the MS.

The gas feed line was switched between a H_2/He (back-transient phase) and a CO/Ar/H_2/He mixture (build-up phase) with constant volumetric flow rate. During the build-up phase, the reactants flow into the catalyst bed, adsorb on the catalyst and the reaction starts, while in the back-transient phase, remaining intermediates are hydrogenated to products and can desorb. Ar acts as an internal standard, representing the RTD for each up- and downward switching event. At the reactor outlet, additionally H_2 and Ne was added. H_2 acts as a dilution to minimize the residence time in the tubing after the reactor and to ensure more consistent ionisation in the MS measurement. Due to the known molar flow rate of the external standard Ne, the total molar flow rate can be derived from the measured molar fractions from the MS.

Evaluation of the Catalytic Experiments

After 25 switching periods, the system reaches the limit cycle in which the individual periods are identical. Hence, averaging over those periods and applying statistical analysis provides a very narrow confidence interval and a high statistical significance of the transient step response. From the physical perspective the invariance of the periodic response during the limit cycle means that all observed transient phenomena are reversible.

The catalytic experiments were evaluated calculating the absolute and transient molar flow rates, $\dot{n}_{i,\mathrm{abs}}$ and $\dot{n}_{i,\mathrm{trans}}$, respectively. The measured ionic currents from the MS were converted via calibration into molar fractions. Via eq. (1), the total outlet molar flow rate, $\dot{n}_{\mathrm{tot}}$, is calculated from the measured molar fraction and known molar flow rate of the external standard Ne, x_{Ne} and $\dot{n}_{\mathrm{Ne}}$, respectively. By that, also the non-equimolarity of the reaction is considered and the outlet molar flow rates of all other components can be calculated by eq. (2).

$$\dot{n}_{\mathrm{tot}} = \frac{\dot{n}_{\mathrm{Ne}}}{x_{\mathrm{Ne}}} \tag{1}$$

$$\dot{n}_{i,\mathrm{abs}} = x_i\, \dot{n}_{\mathrm{tot}} \tag{2}$$

From the molar flow rates and the measured RTD function, F_{Ar}, of the internal standard Ar (see eq. (3)), a theoretical step response, $\dot{n}_{i,\mathrm{theo}}$, for each species is calculated (eq. (4)). This represents the response in case that the steady-state kinetics apply for the transient operation, as well, with $\dot{n}_{ss_\uparrow}$ and $\dot{n}_{ss_\downarrow}$ as upper and lower reference values, i.e. the molar flow rates directly before each of both switching events.

$$F_{\mathrm{Ar}} = \frac{\dot{n}_{\mathrm{Ar}}(t) - \dot{n}_{\mathrm{Ar,ss}_\downarrow}}{\dot{n}_{\mathrm{Ar,ss}_\uparrow} - \dot{n}_{\mathrm{Ar,ss}_\downarrow}} \tag{3}$$

$$\dot{n}_{i,\mathrm{theo}}(t) = F_{\mathrm{Ar}}(t) \cdot \left(\dot{n}_{i,\mathrm{ss}_\uparrow} - \dot{n}_{i,\mathrm{ss}_\downarrow}\right) + \dot{n}_{i,\mathrm{ss}_\downarrow} \tag{4}$$

From the difference between the measured and the theoretical molar flow rates, the so called transient molar flow rate is calculated, see eq. (5).

$$\dot{n}_{i,\mathrm{trans}} = \dot{n}_{i,\mathrm{theo}} - \dot{n}_{i,\mathrm{abs}} \tag{5}$$

Here, $\dot{n}_{i,\mathrm{trans}}$ represents the accelerated (or decelerated) response of compound i with respect to the expected response according to the RTD and steady-state reaction kinetics. The main reasons for these deviations are interactions of the gaseous compound with the catalyst surface through ad-/desorption and surface reactions. With these transient molar flow rates, the component and elemental balance over the catalyst surface can be drawn, according to eqs. (6) (component) and (7) (elemental):

$$\frac{dn_{i,\mathrm{surf}}}{dt} = -\dot{n}_{i,\mathrm{trans}} \tag{6}$$

$$n_{h,\mathrm{surf}} = \sum_i \beta_{h,i} n_{i,\mathrm{surf}} \text{ and } \dot{n}_{h,\mathrm{surf}} = \sum_i \beta_{h,i} \dot{n}_{i,\mathrm{surf}} \tag{7}$$

With $n_{i,\mathrm{surf}}$ and $n_{h,\mathrm{surf}}$ as the molar amount of species i and element h on the surface and $\beta_{h,i}$ as the number of atoms of element h in species i. More detailed information on the evaluation is described by Meyer et al.[26].

Results and Discussion

Steady-state experiments

To determine suitable operating points for the PTK experiments, we first performed several steady-state experiments. We varied the pressure between 2 and 6 bar, the temperature between 220 and 280 °C and the H_2:CO-ratio between 2 and 6. The respective conditions, as well as hydrocarbon selectivities are shown in table 2. GC measurements show absence of CO_2 formation, therefore we assume only negligible water-gas shift activity. The hot and cold trap at the reactor outlet remained empty for all operating points, even after several days of operation. Therefore, we also assume that the formation of liquid hydrocarbons is negligible. As operating point 10 (see table 2) exhibits the lowest selectivity towards longer hydrocarbons, but still has a high enough selectivity for $C_{2\text{-}4}$, this operating point was chosen for the PTK experiments. The respective volumetric flow rates through the

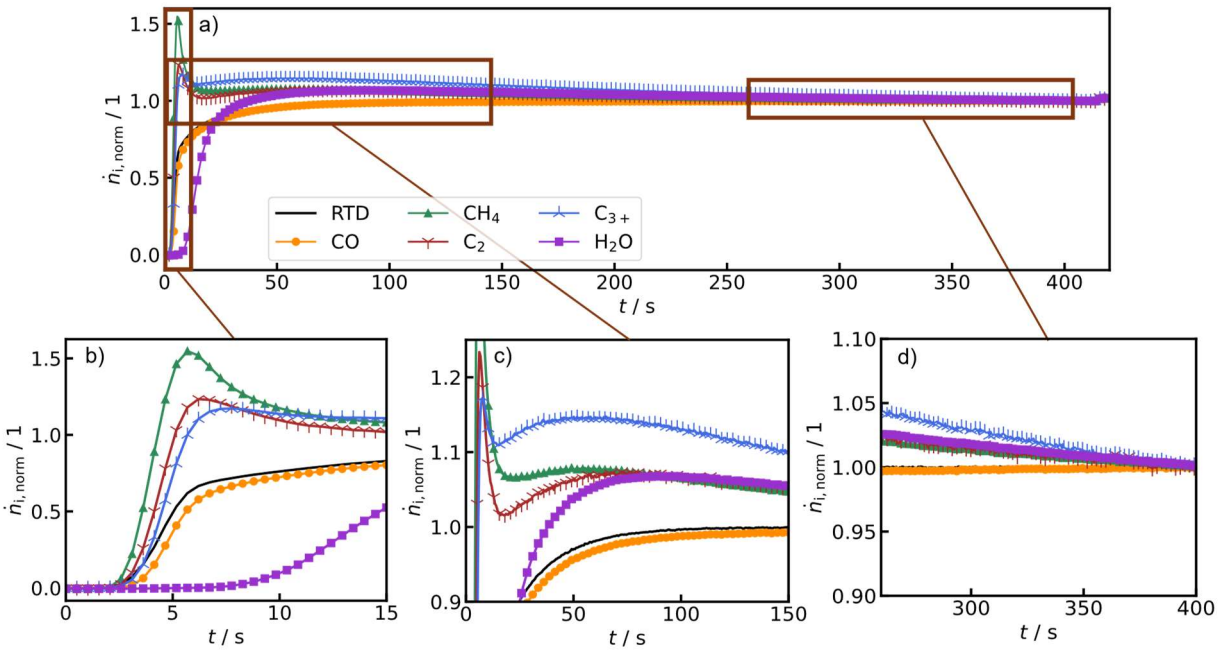

Fig. 1 a): Molar flow rates of CO, CH_4, C_2, C_{3+} and H_2O during the build-up phase at a build-up duration of 7 min and a back-transient duration of 10 min, normalized to the formation rates at the end of the build-up phase (Operating point 10). Subfigures b), c) and d) show zoomed results according to the time axis.

Table 2: Conditions and hydrocarbon selectivities, S_i, during steady-state experiments.

Operating Point	p / bar	T / K	H_2/CO	S_{CH_4} / 1	$S_{C_{2-4}}$ / 1	$S_{C_{5+}}$ / 1
1	6	493	2	0.84	0.109	0.051
2	6	493	3	0.83	0.120	0.050
3	6	513	4	0.81	0.146	0.044
4	6	533	4	0.82	0.147	0.033
5	6	533	6	0.86	0.121	0.019
6	4	533	4	0.85	0.131	0.019
7	4	533	6	0.88	0.108	0.012
8	6	553	6	0.85	0.135	0.015
9	6	553	4	0.84	0.147	0.013
10	4	553	4	0.85	0.145	0.005

reactor are shown in table 3. Since operating point 10 provides a CO conversion of 6.5 % we assumed differential conditions, where only negligible concentration gradients in the catalyst bed are present. Hence, a CSTR balance is appropriate for evaluation.[30]

Table 3: Volumetric flow rates, $\dot{V}_i$, used for the PTK experiments during the build-up phase. During the back-transient phase CO and Ar were replaced by He. STP: at standard temperature and pressure.

$\dot{V}_{H_2}$ / $ml_{STP}\ min^{-1}$	$\dot{V}_{CO}$ / $ml_{STP}\ min^{-1}$	$\dot{V}_{He}$ / $ml_{STP}\ min^{-1}$	/	$\dot{V}_{Ar}$ / $ml_{STP}\ min^{-1}$
72	18	28		2

PTK experiments – Build-up phase

In fig. 1, the step responses in the limit cycle of the reactant CO and the products CH_4, C_2, C_{3+} and H_2O during the build-up phase are shown. Note that the results are normalized to the values at the end of the build-up phase for each individual species. As seen here, the carbonaceous products exhibit a strong overshoot over the steady-state formation rate as represented from the RTD behavior, shown in the black line (see b). CH_4 exhibits the highest overshoot with around 1.55 times the steady-state formation rate in the maximum, followed by C_2 and C_{3+} with 1.23 and 1.17 times the steady-state formation rate, respectively. CH_4 increases the fastest, after which C_2 and the C_{3+} start to increase subsequently and also reach the maximum slightly later. C_2 and C_{3+} show a second maximum (see c) after around 1 min of time on stream (TOS), after which all species then decrease slowly to the steady-state value, while the decrease is slower, the higher the carbon number is, as seen in figure 1 d).

In contrast, the response of CO is slightly delayed compared to the RTD, while H_2O first appears several seconds later, when the other products already start to decrease again. This indicates a significant storage amount of carbon and oxygen on the catalyst surface, which will be discussed in detail later. In a previous investigation with the same catalyst under CO_2 methanation conditions, it was observed that the TiO_2 support has a high adsorption capacity for H_2O.[28] Hence, we also assume that the delay in the H_2O molar flow rate is caused by its adsorption on the support material.

The overshoot for CH_4 is already well known from literature and is caused by the inhibiting effect of CO on the reaction rate, while the first overshoot for C_2 and C_{3+} are attributed to the same effect. At the beginning of the build-up phase, the catalyst surface is covered with hydrogen, which is then slowly displaced by adsorbing CO, therefore inhibiting the reaction rate after passing through an optimal ratio between H:CO on the surface.[10,23]

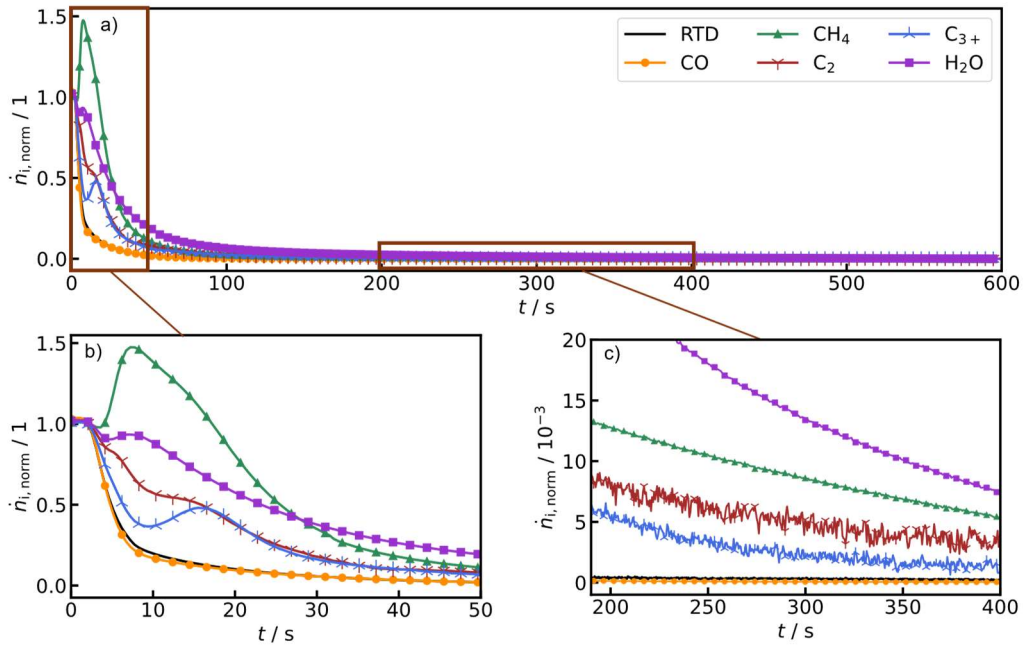

Fig. 2 a): Molar flow rates of CO, CH_4, C_2, C_{3+} and H_2O during the back-transient phase at a build-up duration of 7 min and a back-transient duration of 10 min, normalized to the formation rates at the end of the build-up phase (Operating point 10). Subfigures b) and c) show zoomed results according to the time axis.

The inhibiting effect explains the initial overshoot and fast decrease, whereas we attribute the second maximum for C_2 and C_{3+} as well as the subsequent slow decrease to a different effect. Our previous investigations on Ni showed that the inhibiting effect of CO settles quickly after several seconds.[10] Therefore, we assume that the slow decrease is due to accumulation of a less active carbon species on the surface, which blocks adsorption sites for H_2, but can participate as an intermediate in the hydrocarbon chain formation. Hence, a maximum for the production of C_2 and C_{3+} occurs, when the surface coverage with carbonaceous intermediates is optimal.

In the limit cycle, the formation of the surface species is fully reversible. Thus, the accumulation of a less active carbon species is reversible by the hydrogenation of the blocking species in the following back-transient phase. The presence of several different carbon species, i.e., C_α and C_β, was already proposed in literature[20,21,31–33] and will be discussed in detail later.

PTK experiments – Back-transient phase

After switching back to H_2/He, the back-transient phase starts, which is shown in fig. 2. We still see a formation of products several seconds to minutes after the switch, which corresponds to the stored carbon and oxygen during the build-up phase, as the CO in the gas phase approaches zero within the first minute after the switch. Additionally, CO decreases faster than the RTD, which corresponds to an increased consumption after the switch. At the same time, we see a repeated overshoot over the steady-state formation rate in CH_4, coinciding with a maximum in the H_2O molar flow rate. We conclude that when the adsorption sites, which are previously blocked by CO become available again, the reaction rate starts to increase drastically, consuming additional CO from the gas phase and forming mainly CH_4 and H_2O.[10,23]

For the C_2 and C_{3+} components, the molar flow rates also progress above the values expected from the RTD, indicating the hydrogenation of surface intermediates, even after CO hast been flushed out of the reactor. Furthermore, these hydrocarbons exhibit a second and simultaneous maximum around 15 s after the initial overshoot of CH_4, which we attribute to the hydrogenation of the less reactive C_β accumulated in the build-up phase.

Varied Build-up Duration

To investigate the impact of the accumulated C_β species on the back-transient response, we performed experiments with different build-up durations, while keeping the back-transient phase unchanged. The variation of the build-up duration has a significant impact on the back-transient phase (fig. 3), whereas the temporal profile of the build-up phase remains unaffected (see SI: fig. S2). Note that the results denoted by 4 h are obtained from a single shutdown after a 4 h steady-state experiment. The nearly identical build-up behavior shows that the back-transient duration of 10 min is enough to reach the same initial surface state for the build-up phase. This means that the limit cycle is governed by fully reversible interactions between gas phase molecules and the surface.

In fig. 3, the transient molar flow rates (see eq. (5)) of all relevant components are shown. For CO (see fig. 3d), we see negative transient molar flow rates, as expected from increased consumption after the switch to H_2. The build-up duration does not influence the back-transient behavior of CO and H_2O significantly, see SI fig. S5. In contrast, for the carbonaceous products, the longer the build-up duration is, the higher the maximal transient molar flow rates in the back-transient phase are.

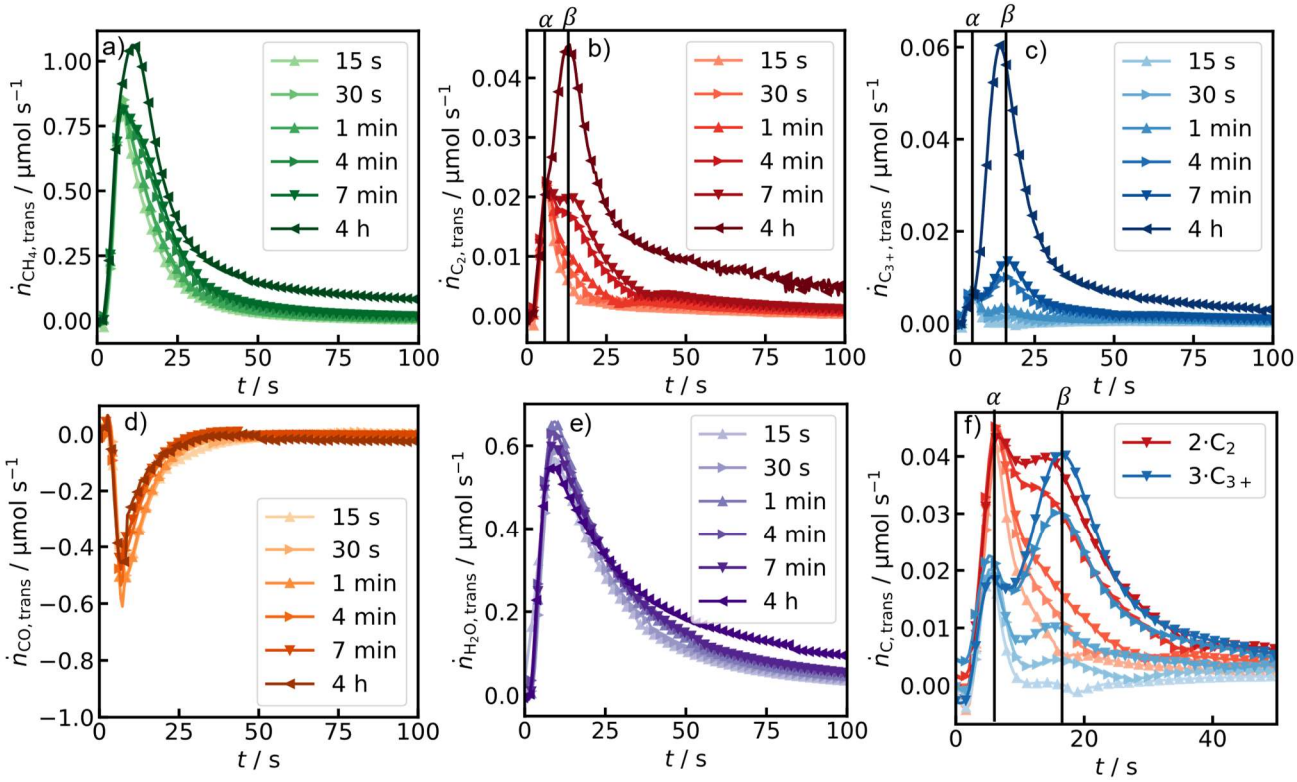

Fig. 3: Transient molar flow rates during the back-transient phase of a) CH_4, b) C_2, c) C_{3+}, d) CO and e) H_2O after a varied build-up duration of 15 s, 30 s, 1 min, 4 min, 7 min and 4 h, as well as f) transient molar flow rates of C_2 and C_{3+} scaled to the number of carbon atoms for the different build-up durations (Operating point 10).

For CH_4 and short build-up durations below 7 min (fig. 3a), the peak of the transient molar flow rate broadens, while the maximum stays approximately at the same position. For the build-up duration of 4 h the maximum shifts slightly in time. The signal of C_2 (fig. 3b and f) shows one single peak for short build-up durations of 1 min and below, which is broadening and develops a shoulder and even a second peak for increasing durations. After 4 h, the first α-peak merges with the second β-peak. For C_{3+} (fig. 3c and f), a similar behavior is observed. However, the α-peak is much less pronounced compared to C_2, while the increase of the β-peak is more pronounced (compare fig. 3b and c).

In fig. 3f, the transient molar flow rates for C_2 and C_{3+} are shown again, scaled to the number of carbon atoms in the molecule. Here, we see that the α-peak is unaffected by the varied build-up duration. Additionally, the β-peak is completely absent for a build-up phase of 15 s. From these results, we conclude that the less reactive species C_β builds up slowly on the catalyst surface, since the β-peak is only visible for longer build-up durations (> 15 s TOS for C_3 and > 1 min for C_2). Furthermore, we assume that C_β blocks active sites for other species, as the overall reaction rate decreases with increasing build-up duration (see also fig. 1). At the same time C_α is formed almost immediately after the switching event and the C_α coverage is unaffected by C_β, since the height of the α-peak stays almost constant for all build-up durations. Hence, we suspect different adsorption sites for both carbon species. Furthermore, C_β takes part in the chain growth reaction, as the increase of the respective peak in the back-transient phase is most pronounced for C_2 and C_{3+}. However, the hydrogenation of C_β to CH_4 is also possible, as the transient molar flow rate of CH_4 is also increasing with raising build-up duration.

The nature of the involved surface carbon species was discussed by Vasiliades et al.[20,21], by combining SSITKA and operando DRIFTS measurements. Here, three different carbon species were observed: highly reactive C_α consisting of adsorbed CO and CH_x intermediates, less reactive C_β consisting of C_xH_y intermediates, as well as an inert C_γ species, consisting of polymeric carbon, which contributes to deactivation and is only hydrogenated at higher temperatures.[20,21] This supports our hypothesis, that C_β is involved in the chain growth reaction, while C_α mainly contributes to the CH_4 formation. The C_γ formation is irreversible under the present conditions and even slower than that of C_β. Hence, the investigation of C_γ requires an adaption of the PTK method and the evaluation of consecutive periods before the limit cycle is achieved. However, we suspect a gradual conversion of C_β to C_γ over time, as the decrease of reaction rate due to C_β accumulation smoothly transitions to a deactivation in longer steady-state experiments.[34]

Elemental surface balance

For quantification of C_α and C_β surface species, we assume the following: 1. The amount of C_α remains constant, due to negligible effect of the build-up duration on the α-peak. 2. For short build-up durations of 15 s or below the transient molar flow rates of C_n species are representative for the hydrogenation of C_α species, since the β-peak is completely absent. These assumptions allow us to determine the transient molar flowrates for the C_α and C_β species (eqs. (8) and (9)).

$$\dot{n}_{i,\mathrm{trans},C_\alpha} = \dot{n}_{i,\mathrm{trans}}(t_{\mathrm{BU}} = 15\ \mathrm{s}) \quad (8)$$

$$\dot{n}_{i,\mathrm{trans},C_\beta} = \dot{n}_{i,\mathrm{trans}} - \dot{n}_{i,\mathrm{trans},C_\alpha} \quad (9)$$

With *i* relating to carbon containing components here. In fig. 4, the transient molar flow rates calculated for C_α and C_β as well as those measured for C_2 and C_{3+} during the back-transient phase are shown for the case of a build-up duration of 7 min (see SI fig. S3 and S4 for additional build-up durations and CH_4). Based on the underlying assumptions, it can be seen that C_α is hydrogenated immediately after the switch, while C_β is hydrogenated later on during the back-transient phase.

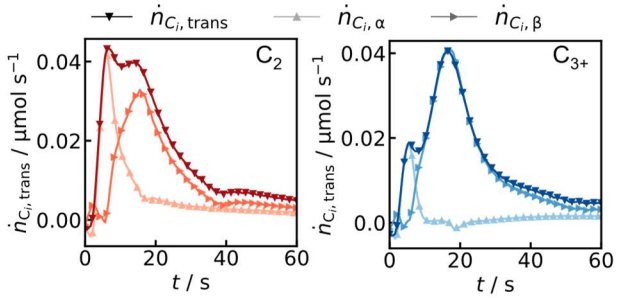

Fig. 4: Transient molar flow rates of C_α and C_β contributing to the transient molar flow rate, $\dot{n}_{\mathrm{trans}}$, of C_2 and C_{3+} during the back-transient phase after a build-up duration of 7 min.

The results for desorbing C_α and C_β are summarized in fig. 5. The results in fig. 5. correspond to the values obtained from the transient molar flow rates during the back-transient phase. There, we assume the amount of C_α to be constant, whereas the amount of C_β increases non-linearly to 97 µmol/g_{cat} after 420 s TOS. After 4 h the amount of C_β even reached 400 µmol/g_{cat}. Again, we assume that C_β refers to accumulation of FT intermediates[20,21] on the surface.

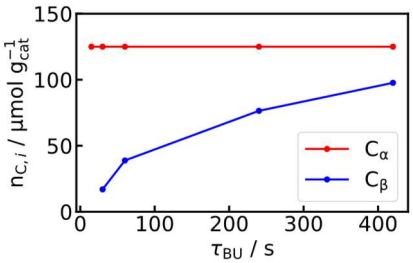

Fig. 5: Amount of C_α and C_β desorbing from the catalyst surface as function of the duration of the build-up phase τ_{BU}, calculated by integration of eqs. (8) and (9).

Conclusions

The hydrogenation of CO on a Co/TiO_2 catalyst under transient conditions was investigated experimentally using the PTK method. By switching between synthesis gas and hydrogen and measuring the transients between the two operating points, the amount of carbon stored on the catalyst surface was evaluated based on material balances. An internal standard enabled the separation between residence time and kinetic effects on the measured transient response. By varying the build-up duration, the amount of carbon accumulated at the surface was affected, which led to the following main conclusions, illustrated in fig. 6:

1. There are at least two carbon species of different reactivity present on the catalyst surface, namely C_α and C_β.
2. C_α is highly reactive and is formed in the first seconds of the build-up phase. C_α is responsible for the initial overshoot in the response of hydrocarbons during the back-transient phase and exhibits a coverage independent from the build-up duration.
3. C_β is formed slowly and retarded compared to C_α. C_β accumulates on the surface and indirectly leads to blocking of active sites and an overall decrease of the reaction rate over time, since it may be an intermediate for the formation of inactive C_γ species.
4. C_β is involved in the chain growth mechanism in both the build-up and the back-transient phase. With increasing reaction times under synthesis gas, the C_β species becomes the governing intermediate for chain growth.

With the PTK method, we were able to distinguish between C_α and C_β as well as to quantify the molar amounts of both species under transient conditions. With this data, we are able to discriminate a micro-kinetic model for CO hydrogenation into hydrocarbons in upcoming work.

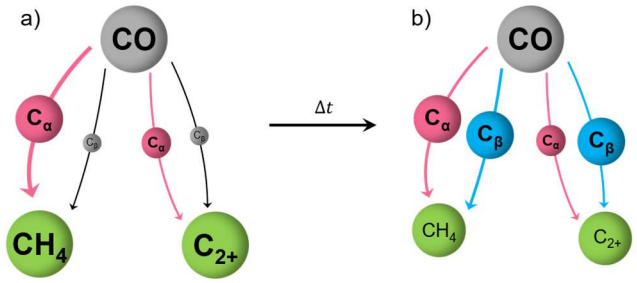

Fig. 6: Illustration of the accumulation of C_β and its effect on the reaction. a) represents the beginning of the build-up phase with primarily C_α on the surface, reacting predominantly to CH_4. b) represents the end of the build-up phase. C_β, reacting predominantly to C_{2+}, accumulates on the catalyst surface, leading to blocking of active sites for other reactants, e.g. H_{ad}, decreasing the overall reaction rate over time.

Supporting Information

In the supporting information we provide additional data for the catalyst characterization, the dynamic experiments and the separation of C_α and C_β.

Acknowledgements

We thank DFG for funding in the framework of the Priority Programme 2289 Hetero-Aggregates (project MA3333/25-1).

Keywords: transient kinetics • CO hydrogenation • chain growth • heterogeneous catalysis • cobalt catalyst

References

[1] C. Schnuelle, J. Thoeming, T. Wassermann, P. Thier, A. Von Gleich, S. Goessling-Reisemann, *Energ. Res. Soc. Sci.* **2019**, *51*, 187–197.
[2] R. Daiyan, I. MacGill, R. Amal, *ACS Energy Lett.* **2020**, *5*, 3843–3847.
[3] M. Martinelli, M. K. Gnanamani, S. LeViness, G. Jacobs, W. D. Shafer, *Applied Catalysis A: General* **2020**, *608*, 117740.
[4] K. T. Rommens, M. Saeys, *Chem. Rev.* **2023**, *123*, 5798–5858.
[5] R. Munirathinam, D. Pham Minh, A. Nzihou, *Ind. Eng. Chem. Res.* **2018**, *57*, 16137–16161.
[6] J. Wentrup, G. R. Pesch, J. Thöming, *Renew. Sust. Energ. Rev.* **2022**, *162*, 112454.

[7] A. Duerksen, J. Thiessen, C. Kern, A. Jess, *Sustain. Energy Fuels* **2020**, *4*, 2055–2064.
[8] H. Gruber, P. Groß, R. Rauch, A. Reichhold, R. Zweiler, C. Aichernig, S. Müller, N. Ataimisch, H. Hofbauer, *Biomass Conv. Bioref.* **2021**, *11*, 2281–2292.
[9] K. F. Kalz, R. Kraehnert, M. Dvoyashkin, R. Dittmeyer, R. Gläser, U. Krewer, K. Reuter, J. Grunwaldt, *ChemCatChem* **2017**, *9*, 17–29.
[10] D. Meyer, J. Friedland, J. Schumacher, M. G. Gäßler, R. Güttel, *Chemical Engineering Science* **2022**, *250*, 117405.
[11] M. Langer, D. Kellermann, H. Freund, *Chem. Eng. J.* **2023**, *467*, 143217.
[12] R. Zhang, Y. Wang, P. Gaspard, N. Kruse, *Science* **2023**, *382*, 99–103.
[13] B. Zijlstra, R. J. P. Broos, W. Chen, I. A. W. Filot, E. J. M. Hensen, *Catalysis Today* **2020**, *342*, 131–141.
[14] R. Chacko, K. Keller, S. Tischer, A. B. Shirsath, P. Lott, S. Angeli, O. Deutschmann, *J. Phys. Chem. C* **2023**, *127*, 7628–7639.
[15] R. J. Berger, F. Kapteijn, J. A. Moulijn, G. B. Marin, J. De Wilde, M. Olea, D. Chen, A. Holmen, L. Lietti, E. Tronconi, Y. Schuurman, *Appl. Catal. A* **2008**, *342*, 3–28.
[16] P. Janssens, J. Poissonnier, A. Chakkingal, R. Bos, J. W. Thybaut, *Catalysis Communications* **2023**, *179*, 106688.
[17] W. Chen, B. Zijlstra, I. A. W. Filot, R. Pestman, E. J. M. Hensen, *ChemCatChem* **2018**, *10*, 136–140.
[18] W. Chen, I. A. W. Filot, R. Pestman, E. J. M. Hensen, *ACS Catal.* **2017**, *7*, 8061–8071.
[19] M. A. Vasiliades, C. M. Kalamaras, N. S. Govender, A. Govender, A. M. Efstathiou, *J. Catal.* **2019**, *379*, 60–77.
[20] M. A. Vasiliades, K. K. Kyprianou, N. S. Govender, A. Govender, R. Crous, D. Moodley, A. M. Efstathiou, *Catalysts* **2020**, *10*, 583.
[21] M. A. Vasiliades, N. S. Govender, A. Govender, R. Crous, D. Moodley, T. Botha, A. M. Efstathiou, *ACS Catal.* **2022**, *12*, 15110–15129.
[22] W. Chen, R. Pestman, B. Zijlstra, I. A. W. Filot, E. J. M. Hensen, *ACS Catal.* **2017**, *7*, 8050–8060.
[23] A. Bundhoo, J. Schweicher, A. Frennet, N. Kruse, *J. Phys. Chem. C* **2009**, *113*, 10731–10739.
[24] A. Raub, H. Karroum, M. Athariboroujeny, N. Kruse, *Catal Lett* **2021**, *151*, 613–626.
[25] M. Athariboroujeny, A. Raub, V. Iablokov, S. Chenakin, L. Kovarik, N. Kruse, *ACS Catal.* **2019**, *9*, 5603–5612.
[26] D. Meyer, J. Friedland, J. Schumacher, R. Güttel, *Chemical Engineering Research and Design* **2021**, *173*, 253–266.
[27] J. Stahl, J. Ilsemann, S. Pokhrel, M. Schowalter, C. Tessarek, A. Rosenauer, M. Eickhoff, M. Bäumer, L. Mädler, *ChemCatChem* **2021**, *13*, 2815–2831.
[28] M. Gäßler, J. Stahl, M. Schowalter, S. Pokhrel, A. Rosenauer, L. Mädler, R. Güttel, *ChemCatChem* **2022**, *14*, e202200286.
[29] D. Meyer, J. Schumacher, J. Friedland, R. Güttel, *Ind. Eng. Chem. Res.* **2022**, *61*, 2045–2054.
[30] S. O. Shekhtman, G. S. Yablonsky, *Ind. Eng. Chem. Res.* **2005**, *44*, 6518–6522.
[31] A. M. Efstathiou, C. O. Bennett, *Chemical Engineering Communications* **1989**, *83*, 129–146.
[32] P. Winslow, *Journal of Catalysis* **1985**, *91*, 142–154.
[33] J. Barrientos, M. Lualdi, M. Boutonnet, S. Järås, *Applied Catalysis A: General* **2014**, *486*, 143–149.
[34] M. Gäßler, R. Güttel, J. Friedland, **2024**, DOI 10.26434/chemrxiv-2024-2fqn7.